Proceedings Paper:
Zhaoyuan, L., Chan, L., Walters, N. et al. (4 more authors) (2018) Structural health monitoring using magnetostrictive sensors. In: 2018 IEEE International Magnetic Conference (INTERMAG). 2018 IEEE International Magnetics Conference (INTERMAG), 23-27 Apr 2018, Singapore, Singapore . IEEE . ISBN 9781538664254

https://doi.org/10.1109/INTMAG.2018.8508360

Structural Health Monitoring using Magnetostrictive Sensors

LEONG Zhaoyuan[1], Louise CHAN[1], Nicholas WALTERS[1], James CLARKE[1], William HOLMES[1], Simon HAYES[1] and Nicola A. MORLEY[1], Member, IEEE,

[1]Department of Materials Science and Engineering, University of Sheffield, Sheffield, S1 3JD, UK

Polymer composites are used in a wide range of applications including aerospace and automotive. Although they possess good structural properties, they are subjected to complicated modes of failure. This damage is often barely visible, so structural health monitoring of the composite is required to determine when this barely visible damage occurs. This paper presents results on the design and testing of a magnetostrictive actuator for detecting barely visible damage in aircraft composite. Computer modelling was used to design and optimise the actuator. FeSiB ribbon and wires were used as the actuator, co-cured either onto the composite surface or between the composite layers to investigate composite sensitivity to different forms of damage. The actuators were tested for uniform strain, barely visible impact damage, and composite delamination, by measuring the change in magnetisation using a HMC5883L AMR sensor. It was found that the magnetostrictive actuator-AMR sensor together were able to detect all these forms of composite damage.

Index Terms— Magnetostrictive sensors, Composite damage detection, Non-destructive testing

I. INTRODUCTION

CARBON FIBRE reinforced polymer composites are being utilised within aircrafts such as Airbus A350 XWB, due to their good structural properties including high strength to weight ratio, low relative cost compared to substitute materials, high corrosion resistance and complex shape manufacture [1, 2]. Unfortunately one of their main disadvantages is that they are subject to complicated modes of failure, which are difficult to detect and if left too long can lead to irreparable damage [3].

Within the composite, there are three damage mechanisms that occur at different length scales, which are micro-level, macro-level and coupled [4]. The micro-level damage mechanisms focus on the fibre and matrix behaviour and include: fibre fracture, buckling, bending, splitting, and matrix cracking either parallel or perpendicular to the fibre direction. At the macro-level damage mechanisms include manufacturing defects and transverse stress through loading, leading to delamination [5]. All these failure mechanisms will reduce the structural integrity of composite and in the end lead to failure of the part. It is therefore important to monitor composites to detect these failures early enough, so that repair is possible. To do this, sensors which can detect small changes in strain within the composite are required as all the different failure mechanisms lead to an area of increased strain within the composite (which can be detected).

To detect damage within the composite early, structural health monitoring (SHM) is undertaken. There are a range of different SHM techniques which have been developed to detect damage within composites, these include both contact and non-contact methods [6]. Non-contact methods include visual inspection, radiography, and ultrasonic inspection, while contact methods include eddy currents, piezoelectric materials, and optical fibres [7]. Although techniques such as piezoelectric sensors and optical fibres have been shown to detect the different damages within a lab environment, they have limitations for aircraft use, due to the additional weight that occurs by mounting the sensors and wires on the composite components, which can cause further damage to the composite. The optical fibre sensors size range from 40 μm to 125 μm for the Bragg gratings. Strain sensitivity and resolution strongly depends upon the operation frequency and the interrogation method. For example, fibre Bragg gratings have a strain sensitivity range and resolution of 2000 ± 1 μstrain [8, 9]. The main limitations of the optical fibres are they are delicate and so break easily - requiring trained specialists to attach them to the composite, and furthermore needing extra wiring and hardware when being used [8]. For the piezoelectric sensors, the size range is 200 – 840 μm, so are the largest of the SHM sensors. They have a strain sensitivity and resolution of 150 ± 5 μstrain [10]. Their main limitations are the additional weight, along with the sensors depoling over time, such that they have a life-cycle of 5 years. Thus, new SHM techniques are being investigated, such as magnetostrictive wires [11, 12] and ribbons, which can be monitored using handheld sensors, therefore reducing the weight added to the composite. This paper presents research carried out on the viability of amorphous magnetostrictive ribbons and wires as SHM actuators, via both computer simulations and experimental procedures. Actuator readings (and thus, efficacy) were obtained using both an inductance coil and an AMR sensor, with both methods used to evaluate and ensure actuator sensitivity and reproducibility.

II. EXPERIMENTAL PROCEDURE

For the design of the magnetostrictive actuator, FEM modelling was employed using the COMSOL Multiphysics software to determine the strain detection range of magnetostrictive ribbons and wires when placed on the composite surface. This work also investigated different magnetostrictive materials and the difference between wires and ribbons for the actuator. Table 1 gives the parameters used in the modelling. The wires had a diameter of 129 μm, while the ribbons were 20 μm thick and 3mm wide. Fig. 1a shows the basic design of the actuator within the COMSOL model. A mesh survey was carried out to determine the optimum mesh size to computational time required for the model. This was a variable mesh, with the smallest elements being 17 μm in size

978-1-5386-6425-4/18/$31.00©2018 IEEE

around the ribbons and the wires, and increasing in size over the rest of the composite. This meant that the mesh elements were smaller than the ribbon thickness and wire diameter.

TABLE I
COMSOL MODELING PARAMETERS

Parameter	FeSiB	CoSiB	0°, 90°Carbon Fibre/Epoxy Composite
Relative permeability	45000	290000	1
Electrical Conductivity (S/m)	6.6e5	6.4e5	0.004
Thermal expansion (1/K)	7.6e-6	12e-6	2.15e-6
Youngs' Modulus (GPa)	167	137	70
Magnetisation (T)	1.56	0.6	0
Density (kg/m^3)	7180	7590	1600

Composite samples were fabricated from a 2 × 2mm twill weave pre-impregnated carbon fibre epoxy system (VTC401®) from SHD Composites. Four layers/plies of 400 × 450 mm pre-preg (fibre volume fraction between 50-60% and a void content of <1% post cure) were placed on top of each other. The $Fe_{77.5}Si_{7.5}B_{15}$ (FeSiB) magnetostrictive ribbons and wires were mounted on both the surface and within the composite with different grid spacings as sensing elements for the actuator. The epoxy within the pre-preg was used to co-cure the ribbons/wires onto/between the composite layers. The samples were then vacuumed packed and cured for 45 minutes at 120°C. Post-curing, the prepared samples were cut into samples of dimensions 150 × 50 × 1mm for the different damage experiments.

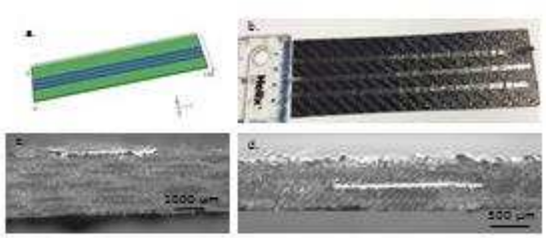

Fig. 1a. COMSOL image of the magnetostrictive sensor: scale mm. b & c. Images of the magnetostrictive ribbon sensors co-cured onto the composite surface and d. image of the ribbon embedded in the composite

From COMSOL modelling, two designs of magnetostrictive actuator where produced (Fig. 1b): Type A had a spacing of 20mm between the ribbons/wires; while Type B had a spacing of 10mm between the ribbons/wires. For each design at least 4 different panels were made up with the actuators attached. To check for repeatability between actuators, the average inductance of each sample was measured using a 112 turn pick-up coil connected to an Atlas LCR45 analyser [12]. The average inductance for type A ribbons were measured as 345±2μH (ribbons) and 259.3±0.5μH (wires), while for type B they were 395±2μH (ribbons) and 261±2μH (wires). Thus there was good repeatability between the actuators. Also the ribbons gave a larger overall inductance compared to the wires. The inductance measurement depends on the volume of the magnetic sample, such that the larger the volume, i.e. for a 15cm length, wire = 1.96 mm^3 and ribbon = 9 mm^3, the larger the inductance response, as observed. It also depends on the permeability and domain structure, which differ between wires and ribbons. The domain structure of the magnetic ribbon or wire depends on the magnetoelastic and magnetostatic energy, and can be manipulated using post-fabrication heat treatment to achieve the "ideal" domain structure for the largest changes in inductance.

Tests were performed to determine if the magnetostrictive actuators could detect composite damage, strain in different conditions and composite delamination. Two methods were used to determine the strain response in the fabricated samples: 1) via inductance measurements using a pick-up coil, and 2) magnetic measurements via an AMR sensor.

The uniform strain sensitivity of the magnetostrictive actuator was tested using the inductance methodology [12]. These were done by straining the composite samples over a range of known bend radii, to determine the change in inductance as a function of strain. The inductance was measured before the composite was strained and under strain, and the difference taken to give a change in induction due to the applied strain. This allows for the sensitivity of the magnetostrictive method to be investigated. Further investigations into the magnetostrictive actuator strain response at different temperatures were also carried out. This involved measuring the uniform strain sensitivity at three different temperatures: 21, -18 and -24°C. The composite was cooled down to the temperature, and uniform strain measurements were taken using the bend radii and the LCR45 analyser.

For the barely visible impact damage (BVID) experiments, a point drop test was carried out, which induced 1.57J of impact damage onto the composite. Both the pick-up coil and the AMR sensor were used to determine the magnetic response before and after impact damage. The inductance along the composite was also measured as a function of distance, to determine the profile of the damage.

Delamination was detected using a HMC5883L AMR sensor controlled by an Arduino microcontroller. In order to verify the usability of the sensor, magnetic readings were taken of Type B samples for comparison when strained on bending rigs of different radii. The change in magnetisation (where the change is defined as the difference between pre-strain and post-strain readings) was detected, with each data point representing the mean of 16 repeats. Delamination was simulated through the addition of diethylenetriamine as a hardener to a secondary epoxy resin layer joining two composite layers fabricated according to the methods outlined above. For these samples, magnetostrictive actuators were co-cured between two composite layers. This procedure ensures that the secondary epoxy layer is weaker than the pre-fabricated samples and so will cause delamination between both composite layers first, before failure of the pre-fabricated samples. The composites were tested on an Instron mechanical testing machine in three-point bending set-up to obtain stress-strain curves concomitantly with the change in magnetisation. Change in magnetisation is measured with an AMR sensor placed on the surface of the composite sample, with three repeats performed for each sample.

III. Results and Discussion

A. COMSOL Modelling

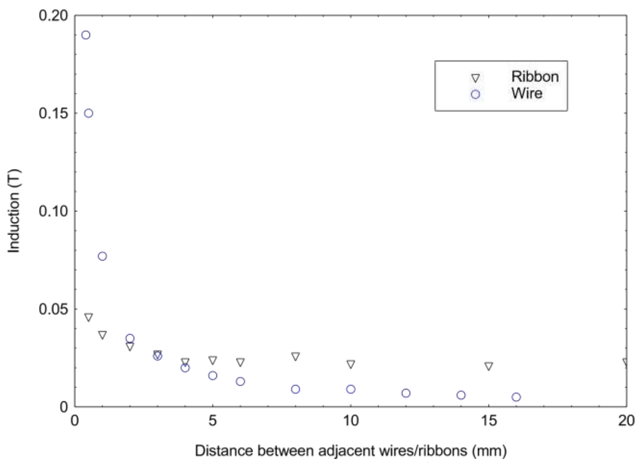

Fig. 2. Magnetic induction as a function of distance between the magnetostrictive wires/ribbons determined from COMSOL modelling

From COMSOL modelling it was determined that for a spacing of 6 mm between adjacent FeSiB wires, the average induction across the surface was 0.012T, while for CoSiB wire the average induction across the surface was 0.006T. The results suggest that the FeSiB wires should have higher strain sensitivity, which is in agreement with experimental results [12]. One of the main differences between FeSiB and CoSiB wires and ribbons is the permeability, which is the change in magnetic induction with applied magnetic field, and is strongly dependant upon the magnetic hysteresis loop. For amorphous magnetic materials, the hysteresis loop is dominated by the shape anisotropy, magnetoelastic anisotropy and their associated domains. For amorphous wires, the domain structure depends on whether the material has a positive (FeSiB) or negative (CoSiB) magnetostriction constant, as it is a competition between the magnetoelastic and magnetostatic energies. FeSiB wires have a core-shell domain arrangement [13], which consists of an inner core, where the magnetisation points along the wires and an outer shell consisting of closure domains, which gives rise to a radial magnetisation. While for CoSiB wires, the inner core is the same, but the magnetisation in the outer shell is circumferential [14]. For the FeSiB ribbon, the domain structure strongly depends on the stress state within the ribbon, as under tensile stress, large wide domains with in-plane anisotropy form, while under compressive stress fine closure domain form with perpendicular anisotropy [15]. Thus for magnetostrictive wires and ribbons, different domain structures arise due to the magnetoelastic and magnetostatic energies, this means each sample will have a different hysteresis loops, which leads to differences in the permeability.

The comparison between wires and ribbons, along with spacing between adjacent wires/ribbons is seen in Fig. 2. The spacing is important as a balance between strain sensitivity and additional weight has to be achieved. It is observed that the average induction across the composite decreases as the spacing increases for both wires and ribbons. For spacings <2mm, the wires have a higher induction compared to ribbons, but this is difficult to achieve experimental, due to wires being 129μm in diameter and thus difficult to place accurately on the composite. At this spacing, the weight of the wire to be added to a 1 × 1m area composite is 52g, which would affect the composite's mechanical properties. For spacings >2mm, ribbons have a higher induction across the composite, which confirms the preliminary experimental results, due to increased surface area being covered vis-à-vis wires.

B. Experimental Results – Inductance coil sensor

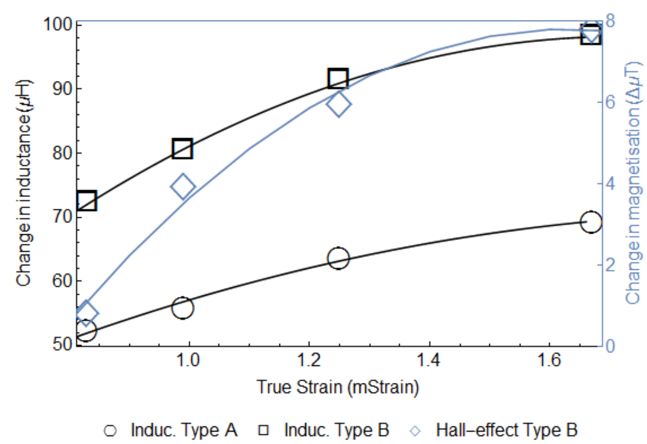

Fig. 3. Applied strain detected via an inductance pick-up coil (data points in black), as well as utilising a Hall-effect sensor (data points in blue).The lines function as a guide for the eye.

For the uniform strain measurements it is observed that there is an increase in the change in inductance with strain (Fig. 3), with the type B design having a larger change compared to the type A design. From this data, the strain sensitivity for each design was determined. For the type A design the strain sensitivity resolution was 25 μstrain and for the type B design, the strain sensitivity resolution was 17 μstrain. Thus as would be expected the design with the smaller ribbons spacing on the composite, had the greater strain resolution. Comparing this to the FeSiB wires previously studied [12], the strain resolution of the ribbons is a factor 10 better than the FeSiB wires (strain resolution = 500 μstrain). This will be due to the increase in the ribbon surface area on the composite compared to the wires. This also confirms the modelling results, which showed that the ribbons should have a better strain resolution. This strain resolution for magnetostrictive actuators is now only an order of magnitude larger than optical fibres and piezoelectric sensors, so are a real alternative for SHM.

For the temperature measurements, it was determined that the magnetostrictive actuator sensitivity decreased as the temperature decreased, but a change in inductance was still measured as a function of strain. At -24ºC, for the type A design, the strain sensitivity resolution was 32 µstrain and for type B design was 24 µstrain. Therefore, the resolution was reduced by ~1.35 compared to sensitivity at 21ºC. It was also determined that the reduction in the inductance with temperature was smaller for ribbon actuators, as compared to wires.

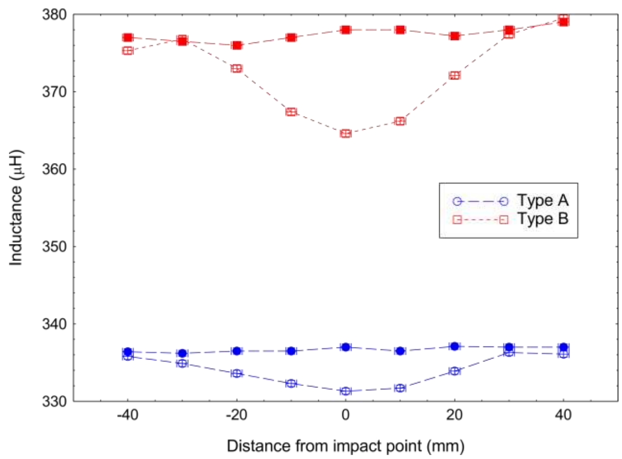

Fig. 4. BVID impact response profile for inductance against distance to impact point. FeSiB ribbons Type A (damage between ribbons) and B (damage on ribbon) configuration. Closed shapes are for no damage and open shapes are for damaged samples.

For the BVID experiments (Fig. 4), it is observed that both designs detected the damage induced. Before BVID, for the undamaged composite (solid shapes), the variation in the inductance was ±2 µH across the length of the composite. For type A orientation, the damage was inflicted between the ribbons, while for type B the damage was inflicted on one of the ribbons. For an impact damage of 1.57J, the change in inductance for the type A design was 6 µH for 1.57J and for type B design was 14 µH, showing that both designs were able to detect BVID. For type A designs, the BVID was ~1cm away from each of the ribbons – this damage was detected by the sensor, demonstrating that a spacing of 2cm between ribbons is sufficient to detect BVID on the composite surface. This is advantageous, as it means that less ribbon will be required to be co-cured onto the composite, so lowering the additional weight added, hence providing a trade-off for the required detection level.

C. Experimental Results – AMR sensor

From Section III-B, the higher sensitivity type B design was employed to test the capabilities of the AMR sensor. The data points obtained following the procedure outline above is presented as an overplot in Fig. 3, shown in blue. The change in magnetisation of the tested samples was found to increase as a function of strain, and the obtained results are found to be comparable to the inductance values obtained previously, giving confidence that the sensor might be used as a method for the detection of composite BVID and delamination.

To further confirm the capabilities of the sensor, impact damage measurements were carried out on the type B design also utilising this sensor, with the ribbons sandwiched between plies 2 and 3. For an impact of 1.63J, the average change in magnetisation was 14µT and for an impact of 3.13J, the average change in magnetisation was 28µT. The measured change in magnetisation is indicative of damage detection utilising the sensor.

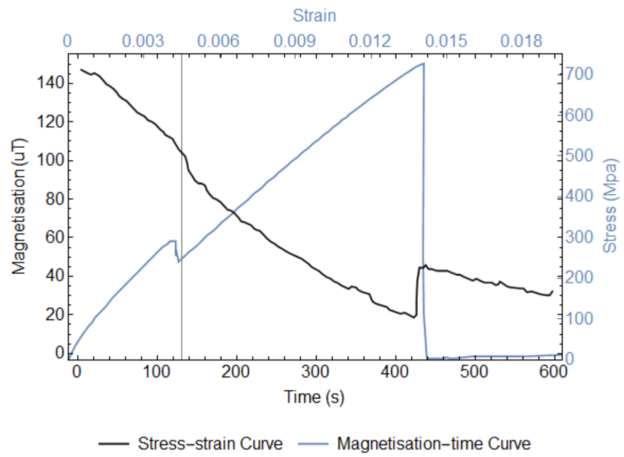

Fig. 5. Overplot of a stress vs. strain curve (in blue) of composite sample, with magnetostrictive ribbons attached and corresponding magnetisation vs. time data (in black) measured simultaneously with the stress-strain curve.

One main damage-type that takes part in composite failure is through delamination. As such, it is important that any sensor design is capable of not only detecting BVID, but also delamination. In order to push sensor capability to its limits, delamination experiments were conducted following the procedure outlined in the methods section. The stress-strain curve of the composite was measured concomitantly with the magnetisation of the magnetostrictive actuator (Fig. 5). It is observed from the stress-strain curve that delamination occurs at a strain of 0.004, which corresponds to a change in the magnetisation gradient at ~140s. At 0.014 strain the sample experiences failure, and this is observed as a large positive jump in the magnetisation. The results were found to be consistent with repeat experiments, demonstrating the ability of a magnetostrictive actuator with an AMR sensor to pick-up and detect a measurable change in magnetisation that corresponds to composite delamination.

IV. CONCLUSIONS

Magnetostrictive actuators made from FeSiB ribbons have been shown to be an effective method of measuring different forms of damage to aircraft composite, including impact and layer delamination (demonstrating good response to measurements via both inductance and AMR sensors). Using magnetostrictive ribbons rather than wires improved the strain resolution by a factor 10. One issue with the inductance coil sensor is the requirement that the composite sample be within the coil. The ability of an AMR sensor to pick up strain, impact damage and delamination is shown here, plus the sensor is used flush against the composite surface. Thus providing a practical method for detecting strain when used in conjunction with magnetostrictive ribbon actuators. These results make them a real alternative to existing structural health monitoring techniques.

ACKNOWLEDGMENT

Part of this research was funded under the Cleansky2 scheme, for the project SHERLOC JTI-CS-2009-01-GRA-01-005

REFERENCES

[1] B. F. Backman, Composite structures, design, safety and innovation, Amsterdam: Elsevier, 2005

[2] V. Giurgiutiu, Structural Health Monitoring of Aerospace Composites, Amsterdam: Elsevier, 2013

[3] C. Soutis "Fibre reinforced composites in aircraft construction", Progress in Aerospace Sciences, pp. 143-151, 2005

[4] R. Talreja, "Damage development in composites: Machanisms and modelling" Journal of Strain Analysis for Engineering Design, vol 24, 2, pp 215-222, 1989

[5] A. C. Garg, "Delamination - a damage mode in composite structures", Engineering Fracture Mechanics, vol 29, 5, pp 557-584, 1998

[6] S. Gholizadeh, "A review of Non-destructive testing methods of composite materials", Procedia Structural Integrity, pp 50-57, 2016

[7] W. Staszewski, S. Mahzan and R. Traynor, "Health monitoring of aerospace composite structures - Active and passive approach", Composite Science and Technology, vol. 69, pp. 1678-1685, 2009

[8] R. Di Sante, "Fibre Optic sensors for structural health monitoring of aircraft composite structures: recent advances and applications", Sensors, vol. 15, pp. 18666-18713, 2015

[9] H Tsutsui, A. Kawamata, T. Sanda and N. Takeda, "Detection of impact damage of stiffened composite panels using embedded small-diameter optical fibers." Smart Material Structures vol 13,. pp 1284-1290 2004

[10] S. G. Taylor, G. Park, K. M. Farinholt and M. D. Todd, "Diagnostics for piezoelectric transducers under cyclic loads deployed for structural health monitoring applications". Smart Material Structures. pp 11. 2013

[11] A. Christopoloulos, E. Hristoforou, I Koulalis and G Tsamasphyros, "Inductive stain sensing using magnetostrictive wires embeded in fibre laminates", Smart Material Structures, vol 23, pp 085035, 2014

[12] A. Al-Taher, R. W. Reiss, A. D. Lafferty, S. A. Hayes, N. Lupu, I. Murgulescu and N. A. Morley, "Magnetostrictive materials for aerospace applications", Journal of Physics: Conference Series, vol 903, pp. 012010, 2017

[13] P. T. Squire and D. Atkinson “Magnetostrictive and Magnetoelastic properties of rapidly quenched wires”, IEEE Trans. Magn. vol. 31, No 2, pp. 1239 – 1248, 1995

[14] P. T. Squire, D. Atkinson, M. R. J. Gibbs and S. Atalay, “Amorphous wires and their applications”, J. Magn. Magn. Mat. vol. 132, pp. 10-21 1994

[15] O. Zivotsky, A. Titov, Y. Jiraskova, J. Bursik, J. Kalbacova, D. Janickovic, and P. Svec, “Full-scale magnetic, microstructural and physical properties of bilayered CoSiB/FeSiB ribbons” Journal of Alloys and Compounds, vol 581, pp. 685-692, 2013